

# Two-pion Bose-Einstein Correlations data analysis for the CMS Pb-Pb nucleon collisions

Zeying Chen<sup>1,\*</sup>, Guanming Liang<sup>2</sup>, Xiaoyue Peng<sup>3</sup> and Aiting Zhao<sup>4</sup>

<sup>1</sup> School of Physics, University of Science and Technology of China, Hefei, Anhui, 230026, China

<sup>2</sup> Dalian Yuming Senior High School, Dalian 116023, China

<sup>3</sup> Wuhan Britain-China School, Wuhan 430022, China

<sup>4</sup> Tianjin Farragut Academy, Tianjin 300042, China

**Abstract.** From the data collected in the Compact Muon Solenoid (CMS) Pb-Pb nucleon collisions experiment, the two-pion Bose-Einstein correlation functions for different combination of same charges and different charges are plotted. The influence of repulsion and attraction through Coulomb interaction between charged pions is reduced after applying the standard Gamow-factor Coulomb correction on Gaussian function  $C(Q_{inv})$ . According to the Yano-koonin-Podgoretski parametrization, the five-dimensional components of the invariant momentum difference between two pions are calculated. One of the five components, the momentum difference in the transverse plane  $Q_T$ , can be further divided into  $Q_{side}$  and  $Q_{out}$ .  $Q_0$ ,  $Q_{long}$ ,  $Q_{side}$  and  $Q_{out}$  were then separately plotted and fitted with the Gaussian function. The sizes of pion source or the effective interferometric source can be extracted from the fitting finally.

## 1 Introduction

### 1.1. Research Background

Particle accelerators became an essential part of physics research in the late 1960 s when scientists first found evidence of the existence of quarks, through the deep inelastic scattering experiments at the Stanford Linear Accelerator Center in 1968. The Large Hadron Collider (LHC) by CERN in Geneva, Switzerland, was the world's largest and highest-energy particle collider at the time it was built in 2008, reaching a world record  $\sqrt{s_{NN}} = 6.5$  TeV per particle beam. The LHC was founded with the expectation that it would provide answers to some of the most fundamental questions in physics, such as the existence of the Higgs boson, supersymmetry, and dark matter. The data analyzed in our research came from the Pb-Pb nucleon collisions in the Compact Muon Solenoid (CMS) experiment, one of the two general-purpose detectors built on the LHC.

Under standard conditions, gluons and quarks are confined within the atomic nucleus due to constant strong interaction. The Quark Gluon Plasma (QGP) refers to the state of matter in which the quarks and gluons are deconfined-free of the strong interaction restraints at extremely high temperature and energy densities. The Quark Gluon Plasma is produced in the laboratory requires by colliding atomic nuclei, which are heated to a temperature well above the Hagedorn temperature  $T_H=150$  MeV (exceeding  $1.66 \times 10^{12}$  Kelvin), at relativistic energy. The produced particles, such as the pions in the CMS Pb-Pb collisions, are in the QGP state.

Deconfinement enables the detection of their kinematic parameters such as momentum.

In the CMS experiment, detectors can locate the origin of tracks to about  $10 \mu\text{m}$  while the typical distance between particles  $\Delta x$  is about 10 fm. since a direct measurement of the distance between the particles is impossible, Heisenberg's uncertainty principle is applied to the calculation of  $\Delta x$ . The probability of having two bosons in the same quantum state is enhanced according to Bose-Einstein statistics which yields  $\Delta x \cdot \Delta p < \hbar$ . For particles with  $\Delta x \approx 10$  fm and  $\hbar \approx 200$  MeV · fm, the approximate  $\Delta p$  measured is about 20 MeV. The measured momenta of pions are used for the calculation of the four-momentum difference  $Q$  and the Bose-Einstein correlation function. This principle can be applied to the calculation of the typical distance between the deconfined elementary particles, quarks, and gluons, within the Quark Gluon Plasma (QGP).

Bose-Einstein correlation exists between identical bosons. Previous related researches have produced the graphs of the correlation function  $C(Q)$  from data collected in different collision experiments, such as the NA35 [1,2], NA44 [3], and NA49 [4] experiments at CERN. In the CMS Pb-Pb collision experiment, the charges, momentum in the transverse plane  $P_t$ , pseudo-rapidity  $\eta$ , and azimuthal angle  $\Phi$  of the scattering  $\pi^+$  and  $\pi^-$  pions were detected and analyzed. The invariant momentum  $Q_{inv}$  of different pion pairs in the same (Signal) and different (Background) events were separately calculated and counted into the functions  $S(Q)$  and  $B(Q)$ . This subsequently produced the Bose-Einstein correlation function  $C(Q)$ , which was refined with the Gamow factor

\* Corresponding author's e-mail: [crozychan98@mail.ustc.edu.cn](mailto:crozychan98@mail.ustc.edu.cn)

Coulomb correction [5,6] and fitted with both the Gaussian and exponential functions. As introduced in [7,8], the invariant momentum difference  $Q_{inv}$  can be divided into three degrees of freedom  $Q_{long}$ ,  $Q_{side}$ , and  $Q_{out}$  in Bertch-Pratt momentum coordinate [9]. According to the Yano-Koonin-Podgoretski parametrization [4], the invariant momentum difference was divided into the five components  $Q_0$ ,  $Q_{//}$ ,  $Q_{\perp}$ ,  $Y_{\pi\pi}$ ,  $K_{\perp}$ .

## 1.2. Novelty

In our analysis, two correlation functions were separately plotted and fitted with the Gaussian function when  $Q_{inv}$  was derived entirely from the positively- charged  $\pi^+$  and from a mixed combination of both positive  $\pi^+$  and negative  $\pi^-$ . The Gaussian-fitted correlation functions of  $Q_{long}$ ,  $Q_{out}$ , and  $Q_{side}$  were subsequently plotted and compared to the results of  $Q_{//}$  and  $Q_0$ . The dependence of  $R$  on  $K_{\perp}$  is also shown in the figures. The results from our analysis of the correlation between randomly selected, identical pions are coherent with the predictions of the Bose-Einstein correlations.

## 2 Data Analysis Method

The correlation function is  $C(Q) = \frac{S(Q)}{B(Q)}$ , where  $S(Q)$  (signal) and  $B(Q)$  (background) are the counts for

$Q_{inv}$  when the particles are randomly selected from the same and different events.

$$C(Q) = C(p_1 - p_2) = \frac{P_2(p_1, p_2)}{P_1(p_1)P_1(p_2)} \quad (1)$$

$Q_{inv}$  is the four-momentum difference and is derived from the following equation:

$$Q_{inv} = p_1^\mu - p_2^\mu = \sqrt{(p_{1x} - p_{2x})^2 + (p_{1y} - p_{2y})^2 + (p_{1z} - p_{2z})^2 - (E_1 - E_2)^2} \quad (2)$$

For eliminating the effect brought by the Coulomb repulsion of identical pions, we have applied the standard Gamow factor for correction:

$$G(\eta) = \frac{\eta}{e^\eta - 1}, \quad \eta = 2\pi \frac{\alpha m_{pion}}{Q_{inv}} \quad (3)$$

where  $\alpha$  is the fine structure constant,  $m_{pion}$  stands for pion mass and  $Q_{inv}$  characterizes the invariant momentum difference.

The uncertainty of the correlation function  $C(Q)$  is calculated with:

$$\frac{\Delta C'}{C'} = \sqrt{\left(\frac{\Delta C}{C}\right)^2 + \left(\frac{e^\eta - 1 - \eta}{e^\eta - 1} \frac{\Delta Q}{Q}\right)^2} \quad (4)$$

where  $C'$  represents the correlation function after Gamow correction. The correlation function is fitted with the Gaussian function:

$$C(Q_{inv}) = 1 + \lambda e^{(-R_i^2 Q_i^2)} \quad (5)$$

$Z$  is set as the collision axis in the CMS experiment and converted from the laboratory to the Center of Mass Reference Frame (CMRF):

$$p'_x = p_x, p'_y = p_y, p'_z = E(-\beta_{pair}\gamma_{pair}) + p_z\gamma_{pair} \quad (6)$$

$$\beta_{pair} = \frac{p_{z1} + p_{z2}}{E_1 + E_2}, \quad \gamma_{pair} = \frac{1}{\sqrt{1 - \beta_{pair}^2}} \quad (7)$$

We then obtain the expressions for  $Q_T$  and  $Q_{long}$  in CMRF:

$$Q_T = (\Delta p_x^2 + \Delta p_y^2)^{\frac{1}{2}} \quad (8)$$

$$Q_L = \sqrt{\frac{(\Delta E\beta_{pair} + (-\Delta p_y^2))^2}{1 - \beta_{pair}^2}} \quad (9)$$

The correlation function can be expressed with  $Q_T$  and  $Q_{long}$ :

$$C(Q_{long}, Q_T) = 1 + \lambda e^{\frac{1}{2}(Q_T^2 R_T^2 + Q_L^2 R_L^2)} \quad (10)$$

$Q_{side}$  and  $Q_{out}$  are the components of  $Q_T$ :

$$Q_{out} = \frac{(p_{1y}^2 p_{2y}^2 + p_{1z}^2 p_{2z}^2)}{\sqrt{((p_{1y} + p_{2y})^2 + (p_{1z} + p_{2z})^2)^2}} \quad (11)$$

$$Q_{side} = \frac{2(p_{1z} p_{2y} - p_{2z} p_{1y})}{\sqrt{((p_{1y} + p_{2y})^2 + (p_{1z} + p_{2z})^2)^2}} \quad (12)$$

Therefore, the correlation function can be expressed with  $Q_{side}$ ,  $Q_{out}$  and  $Q_{long}$ :

$$C(Q_{side}, Q_{out}, Q_{long}) = 1 + \lambda e^{\frac{1}{2}(Q_{side}^2 R_{side}^2 + Q_{out}^2 R_{out}^2 + Q_{long}^2 R_{long}^2)} \quad (13)$$

All  $\lambda$  in correlation functions is the intensity of correlation and  $R_{inv}$ ,  $R_{long}$ ,  $R_{out}$ ,  $R_{side}$  are the parameters which represent the sizes of the pion source or the effective interferometric source size in each component.

## 3 Results and Discussion

Our data analysis is based on the data collected by detectors in the CMS Pb-Pb collisions experiment. Specifically, we analyzed the data in a 400 MB data file consisting of 20000+ events and hundreds of tracks in each event. 1,000,000,000 and 5,000,000,000 random samples of 2-pion combinations were separately taken for same and different events.

For the correlation graphs plotted from the pion combinations with same charge and different charge, those resulting in  $Q < 0.02$  GeV are excluded from the graphs due to the inherent inaccuracy of the data and the final range for them is [0.02 GeV, 0.15 GeV]. The range of the correlation graphs of  $Q_{out}$ ,  $Q_{side}$ , and  $Q_{long}$  is set at [0.01 GeV, 0.20 GeV]. The light green shades in the graphs represent 95% confidence intervals at each value of  $Q$  for different correlation functions.

The fit to the expressions of correlation function is performed using the minimum chi-square method to acquire their parameters. Fig. 1 shows the result of the fit with the parameter  $R_{inv} = (4.3 \pm 0.3)$  fm. Fig. 3 includes the band of 95% confidence intervals with the parameters  $R_{long} = (4.1 \pm 0.3)$  fm,  $R_{out} = (2.8 \pm 0.4)$  fm and  $R_{side} = (3.2 \pm 0.3)$  fm. In Fig. 4,  $R_t = (3.9 \pm 0.3)$  fm and  $R_0 = (2.9 \pm 0.5)$  fm.

Other information is given by the dependency of  $R_{side}$  and  $R_t$  on  $K_{\perp}$ . In Fig. 5, when we divided  $K_{\perp}$  into five intervals in the region  $0.5 < K_{\perp} < 1.0$ ,  $R_{side}$  and  $R_t$  become a function of average pair transverse momentum  $K_{\perp}$ .

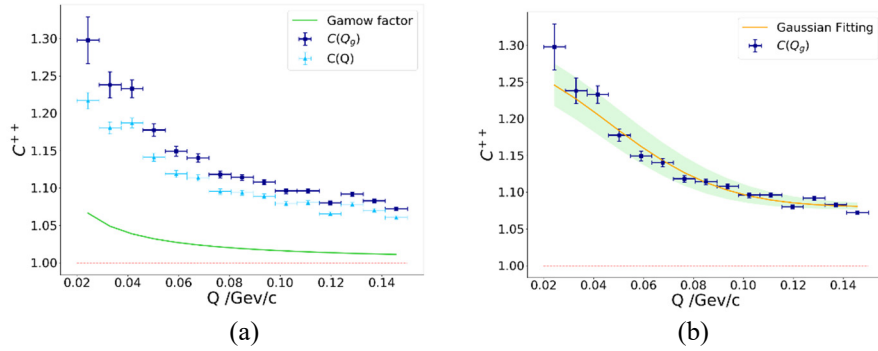


**Fig1.** (a) Correlation graph of 2-pion combinations with positive charge. The effect of the Gamow factor is illustrated with the difference between the sky-blue colored dots  $C(Q)$  and dark-blue colored dots  $C(Q_g)$  before and after the Coulomb correction. The Gamow factor is represented by the green curve; (b) Correlation graph of 2-pion combinations with positive charge. The dark blue dots  $C(Q_g)$  represent the correlation function after the Coulomb correction. The Gaussian fitted curve of  $C(Q)$  is the orange curve.

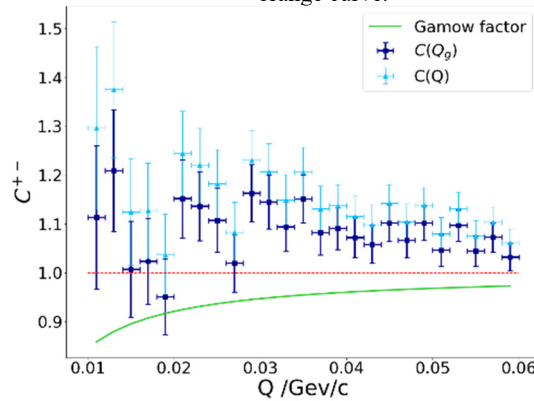


**Fig2.** Correlation graph of 2-pion combinations with different charge. The Gamow factor is the green curve converging to 1 as expected. The effect of Gamow factor is illustrated with the difference between dark-blue colored dots of  $C(Q_g)$  and sky-blue colored dots  $C(Q)$  before and after the Coulomb correction.

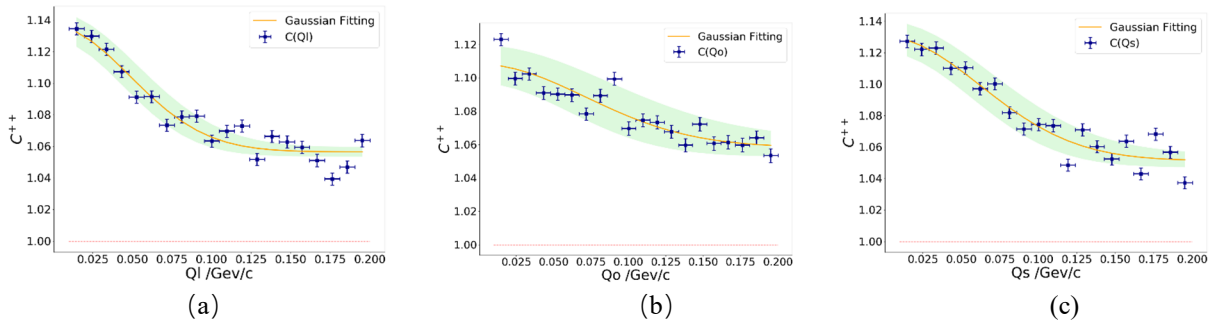


**Fig3.** (a) Correlation graph of  $C(Q_{long})$ ; (b) Correlation graph of  $C(Q_{out})$ ; (c) Correlation graph of  $Q_{side}$ . In both figures, the blue points represent  $C(Q_{long}) / C(Q_{side}) / C(Q_{out})$  after the Coulomb correction and the orange curve represents the Gaussian fitted curves of  $C(Q_{long}) / C(Q_{side}) / C(Q_{out})$ .

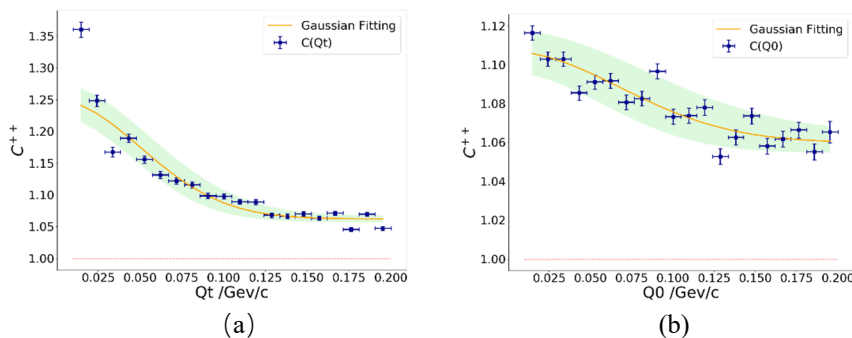


**Fig4.** (a) Correlation graph of the transverse momentum difference  $Q_T$ ; (b) Correlation graph of the energy difference  $Q_0$ . In both figures, the dark blue dots represent the correlation function  $C(Q_T) / C(Q_0)$  after the Coulomb correction. The yellow curve represents the Gaussian fitted curve of  $C(Q_T) / C(Q_0)$ .

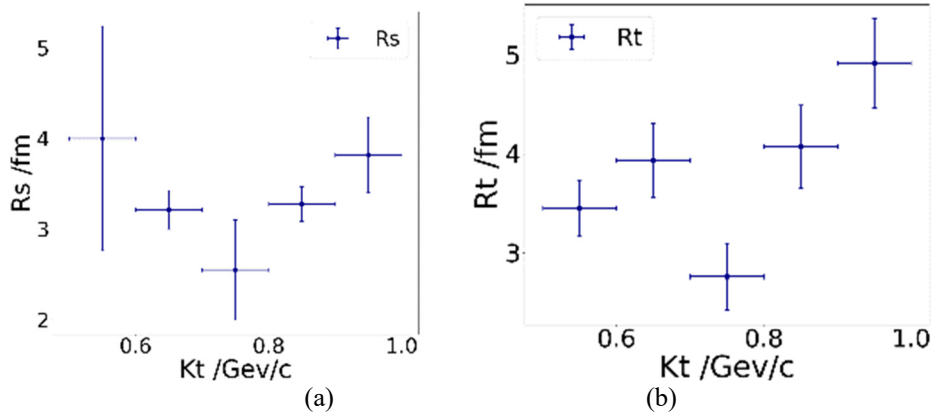


**Fig5.** (a) Relationship of  $R_{side}$  and  $K_{\perp}$ ; (b) Relationship of  $R_t$  and  $K_{\perp}$ .

## 4. Conclusion

A statistical data analysis of the two-pion Bose-Einstein Correlation has been carried out for the CMS Pb-Pb nucleon collisions experiment. The initial graphs of correlation function consist of the charged scenarios for positive-negative, positive-positive, and negative-negative (like previous situation) with three components  $p_x$ ,  $p_y$  and  $p_z$  considering pseudorapidity. The corresponding error bars of the correlation function were added and the correlation function was modified with the standard Gamow-factor Coulomb correction, as well as Gaussian fitting. Z was set as the collision axis in the experiment. The reference frame was converted from laboratory to Center of Mass for the Gaussian fitting of  $Q_{long}$  and  $Q_{out}$ , and  $Q_{side}$ . The invariant momentum difference was calculated from 1 billion random sampling for the same-event scenario and 5 billion random sampling for the different-event scenario. The histogram was divided to obtain discrete correlation function for each Q component.

There was, at maximum, five components of the invariant momentum difference  $Q_{inv}$  in this research, limited by computational capabilities. The results presented in the graphs were influenced by their respective uncertainties. This uncertainty was reduced when the Coulomb correction and the Gaussian fit were applied to the correlation function and more events (1,000 to 20,000) were included in the calculation. The number of bins was then reduced from 45 to 15 or 20. Further research included calculation about the ideal five-dimensional situation with  $Q_t$  (Q Transverse),  $Q_l$  (Q Longitudinal),  $Q_o$  (Q Out),  $Q_s$  (Q Side) and  $Q_0$  (Q Energy), with their dependence on  $K_{\perp}$  (Mean Trans-verse Momentum).

The five-dimensional model still needs to be moderated to produce multi-dimensional histograms with better accuracy in future researches. The data source will be replaced with a larger data file and the random uncertainty reduced, so that we can analyze more components such as  $Y_{\pi\pi}$  and  $\beta_{YK}$ .

## Acknowledgements

We acknowledge the support from Professor Gunther Roland for his guidance and suggestions during our

research on the Bose-Einstein correlations. We acknowledge the support from teaching assistant Kai Jiang for instructions on paper composition.

## References

1. Alber, T. Bchler, J. Bartke, J. Bialkowska, H. & Stefansky, P. (1995). Transverse momentum dependence of bose-einstein correlations in 200a gev/c s+a collisions. *Physical Review Letters*, 74(8), 1303-1306.
2. Roland, G. (1994). Rapidity and transverse momentum dependence of the two -  $\pi$ - correlation function in 200 gev/nucleon s+nucleus collisions. *Nuclear Physics A*, 566(none), 527-530.
3. Bøggild, H., Boissevain, J., Cherney, M., Dodd, J., Downing, J., Esumi, S., ... & Ikemoto, T. (1993). Identified pion interferometry in heavy-ion collisions at CERN. *Physics Letters B*, 302(4), 510-516.
4. Collaboration, N. & Al., H. A. E. (1998). Hadronic expansion dynamics in central pb+pb collisions at 158 gev per nucleon. *The European Physical Journal C - Particles and Fields*, 2(4), 661-670.
5. Alber, T., Baechler, J., Bartke, J., Białkowska, H., Bloomer, M. A., Bock, R., ... & Chan, P. (1995). Two-pion Bose-Einstein correlations in nuclear collisions at 200 GeV per nucleon. *Zeitschrift für Physik C Particles and Fields*, 66(1-2), 77-88.
6. Baym, G. & Braun-Munzinger, P. (1996). Physics of coulomb corrections in hanbury-brown twiss interferometry in ultrarelativistic heavy ion collisions. *Nuclear Physics A*, 610, 286-295.
7. Bertsch, G. F. Gong, M. & Tohyama, M. (1988). Pion interferometry in ultrarelativistic heavy-ion collisions. *Phys Rev C Nucl Phys*, 37(5), 1896-1900.
8. Pratt, & Scott. (1986). Pion interferometry of quark-gluon plasma. *Physical Review D Particles & Fields*, 33(5), 1314.
9. Morita, K. (2006). Rapidity dependence of HBT radii based on a hydrodynamical model. *Brazilian journal of Physics*, 37(3a), 1039-1046.